Weak ferromagnetism and excitonic condensates

M. Y. Veillette and L. Balents

Physics Department, University of California, Santa Barbara, California 93106

We investigate a model of excitonic ordering (i.e., electron-hole pair condensation) appropriate for divalent hexaborides. We show that the inclusion of imperfectly nested electron-hole Fermi surfaces can lead to the formation of an undoped excitonic *metal* phase. In addition, we find that weak ferromagnetism with compensated moments arises as a result of gapless excitations. We study the effect of low-lying excitations on the density of states, Fermi-surface topology, and optical conductivity, and compare to available experimental data.

I. INTRODUCTION

The remarkable discovery of weak ferromagnetism in lightly doped divalent hexaborides has been hailed as a great surprise in the physics of magnetism.[1–7] In spite of the absence of partially filled d or f orbitals, which are usually required for magnetism, these materials undergo a ferromagnetic transition at a relatively high Curie temperature (600 K) and with a small magnetic moment in a narrow range of doping. The authors of Ref. 2 put forward the proposal of a doped excitonic insulator to explain the unexpected ferromagnetism in these materials, a theory that has a long and rich history,[8] but for which hexaborides seem to be the first experimental realization. Band-structure calculations[9] of $D\text{B}_6$ where $D=\text{La,Ba,Sr}$ indicate a small band overlap or small band gap at the three X points in the Brillouin zone, a condition favorable to the formation of an exciton condensate.[10] The Coulomb attraction between particles and holes can overcome the small band gap, and lead to the spontaneous condensation of electron-hole pairs. As a result of Hunds rule, a triplet exciton condensate is energetically favored over a singlet, giving rise to a local-spin polarization within the unit cell but no net magnetization. The connection of exciton condensation to ferromagnetism was first pointed out by Volkov *et al.*[11] Upon doping, a spin-singlet exciton is formed in presence of the triplet order, breaking translational as well as time-reversal symmetry, and hence resulting in ferromagnetism. In more physical terms, the extra carriers added into the system are distributed asymmetrically between the two spin projections to preserve the most favorable pairing condition for one spin orientation.

Although appealing, the excitonic model has been largely studied only for highly idealized cases. In this paper, we relax some of these approximations to extract generic predictions applicable to excitonic condensates. In particular, we are interested in explaining recent angle resolved photo emission spectroscopy (ARPES)[12] measurements and de Haas–van Alphen (dHvA)[13] measurements on the Fermi surface in $\text{Ca}_{1-x}\text{La}_x\text{B}_6$ and SrB_6. We study in some detail the zero-temperature phase diagram as a function of the doping level in the presence of imperfectly nested electron and hole Fermi surfaces. We show that a possible new phase, the excitonic metal (EM), can reconcile the existence of a Fermi surface and an excitonic condensate. Furthermore, as an upshot of the EM, the ungapped Fermi surface leads to a com-

pensated magnetic moment, a mechanism for partial polarization markedly different from the one proposed in Ref. 2.

The paper is structured as follows. First, in Sec. II we introduce a two-band model Hamiltonian, and discuss its physical relevance to the excitonic state. In Sec. III, we analyze the model for the case of perfectly nested Fermi surfaces. Using the techniques of mean-field theory, we recast the problem into a form closely related to BCS theory. In Sec. IV, the effect of incommensurability of the Fermi surface on the emergence of ferromagnetism is studied. We report numerical results on the magnetic moment and density of states in the excitonic phases. The effect of the excitonic order on the optical conductivity is considered in Sec. IV.

II. MODEL

As argued by Balents and Varma,[4] the binding of an electron and a hole is most effective for states with similar group velocities at equal momenta. Hence, in the hexaborides, the electron-hole pair will be more strongly bound if both components are drawn from the same X point of the Brillouin zone. Thus we neglect the three-pocket band structure appropriate to the hexaborides to study a two-band model of conduction and valence electrons. To analyze the problem of excitonic ferromagnetism, we introduce the Green's function defined by the equality

$$\mathcal{G}^{\sigma\sigma'}(\mathbf{r},\mathbf{r}',\tau)=-\langle T_\tau\psi_\sigma(\mathbf{r},\tau)\psi_{\sigma'}^\dagger(\mathbf{r}',0)\rangle. \quad (1)$$

Here $\psi_\sigma(\mathbf{r},\tau)$ and $\psi_\sigma^\dagger(\mathbf{r},\tau)$ are operators annihilating and creating an electron with spin $\sigma\ (=\pm)$ at point $\mathbf{r}$ at imaginary time τ. In the two-band model, we can express the field $\psi_\sigma^\dagger$ in terms of $a_{k,\sigma}^\dagger$ and $b_{k,\sigma}^\dagger$, the creation operator in the conduction and valence bands, respectively:

$$\psi_\sigma(\mathbf{r})=\sum_k \varphi_{a\mathbf{k}}(\mathbf{r})a_{k,\sigma}+\varphi_{b\mathbf{k}}(\mathbf{r})b_{k,\sigma},$$

$$\psi_\sigma^\dagger(\mathbf{r})=\sum_k \varphi_{a\mathbf{k}}^*(\mathbf{r})a_{k,\sigma}^\dagger+\varphi_{b\mathbf{k}}^*(\mathbf{r})b_{k,\sigma}^\dagger, \quad (2)$$

where $\varphi_{a\mathbf{k}}(\mathbf{r})$ and $\varphi_{b\mathbf{k}}(\mathbf{r})$ are the Bloch functions with quasimomentum $\hbar k$ of electrons in the conduction and valence bands, respectively. The Hamiltonian of the system can be written as $H=H_0+H_I$, where

$$H_0 = \sum_{k,\sigma} (\epsilon_k^a - \mu) a_{k,\sigma}^\dagger a_{k,\sigma} + (\epsilon_k^b - \mu) b_{k,\sigma}^\dagger b_{k,\sigma} \qquad (3)$$

is the noninteracting part of the Hamiltonian. ϵ_k^a and ϵ_k^b are the kinetic energy of conduction and valence electrons, respectively. The interacting part of the Hamiltonian is given by the Coulomb interaction

$$H_I = \frac{1}{2} \sum_{\sigma,\sigma'} \int d\mathbf{r}\, d\mathbf{r}'\, \psi_\sigma^\dagger(r) \psi_\sigma(\mathbf{r}) V(\mathbf{r} - \mathbf{r}') \psi_{\sigma'}^\dagger(\mathbf{r}') \psi_{\sigma'}(\mathbf{r}'),$$
$$(4)$$

where $V(\mathbf{r}) = (e^2/\epsilon)(1/|\mathbf{r}|)$. The exciton Bohr radius a_B sets the length scale of the problem, the physics being controlled by momentum exchange processes of the order of $1/a_B$. In the weak binding limit, i.e., when the energy of an exciton E_B is much smaller than the bandwidth E_W, a_B is much larger than the interlattice spacing a and the interaction is dominated by the long-range part of the Coulomb interaction. In this case, we can treat the interaction in the so-called dominant term approximation[2] $H_{DT} = H_0 + \bar{H}_I$, where

$$\bar{H}_I = \frac{1}{2} \sum_{k,k',q,\sigma,\sigma'} V(\mathbf{q}) (a_{k',\sigma'}^\dagger a_{k'-q,\sigma'} + b_{k',\sigma'}^\dagger b_{k'-q,\sigma'})$$
$$\times (a_{k,\sigma}^\dagger a_{k+q,\sigma} + b_{k,\sigma}^\dagger b_{k+q,\sigma}). \qquad (5)$$

Here $V(\mathbf{q}) = 4\pi e^2/\epsilon q^2$ is the long-range part of the Coulomb interaction. Note that, unlike the full crystal Hamiltonian H, H_{DT} *separately* conserves the charge and the spin of the conduction and valence electrons. The order parameter $\langle a_\sigma^\dagger b_{\sigma'} \rangle$ that corresponds to the pairing of a valence and conduction electrons is a matrix in spin space. Because the approximate Hamiltonian separately conserves the particle number of each species, the energy of the system is invariant under a constant shift of the overall phase of the order parameter. Similarly, the SU(2)×SU(2) symmetry leads to the degeneracy of the excitonic triplet and singlet states. The full crystal Hamiltonian will in general break these symmetries. However, we can justify the use of the approximate Hamiltonian by arguing the neglected terms will affect the formation of the excitonic condensate only at a very low-energy scale. Indeed, these terms involve matrix elements of the Coulomb potential at wave vector $\sim 1/a$ and hence can be treated as small perturbations compared to the long-range Coulomb interaction part of the interaction at wavevector $1/a_B$. It is interesting nonetheless to study how they lift the degeneracy. There are three classes of terms that we have ignored. The first one contains electron-hole exchange terms such as $a_{k+q,\sigma}^\dagger a_{k,\sigma'} b_{k'-q,\sigma'}^\dagger b_{k,\sigma}$. These terms break the SU(2)×SU(2) symmetry explicitly. They are ultimately responsible for the splitting of the ground state of the Hamiltonian in favor of the triplet state.[8] Another class of terms left aside are matrix elements of the kind $a_{k+q,\sigma}^\dagger a_{k,\sigma} b_{k'-q,\sigma'}^\dagger a_{k',\sigma'}$. In case of the hexaborides, these terms are prohibited at small k, k', and q due to lattice symmetry. The third class contains interband pair scattering terms that create and destroy simultaneously two valence and conduction electrons in the Brillouin zone. This term will

select the phase of the order parameter. However, the effect of these virtual processes are limited by the low density of excited pairs.

III. MEAN-FIELD APPROACH

First we study the Hamiltonian H_{DT} in a mean-field (MF) treatment. For a large exciton radius a_B, the excitons overlap strongly and we expect MF theory to give correct results. The excitonic phase is characterized by the pairing of valence and conduction electrons. To emphasize the similarity of our treatment to the Nambu-Gorkov formalism for superconductors, we introduce the Green's function in the Bloch basis

$$\mathcal{G}^{\sigma\sigma'}(\mathbf{k},\tau)$$
$$= -\begin{pmatrix} \langle T_\tau a_{k,\sigma}(\tau) a_{k,\sigma'}^\dagger(0) \rangle & \langle T_\tau a_{k,\sigma}(\tau) b_{k,\sigma'}^\dagger(0) \rangle \\ \langle T_\tau b_{k,\sigma}(\tau) a_{k,\sigma'}^\dagger(0) \rangle & \langle T_\tau b_{k,\sigma'}(\tau) b_{k,\sigma'}^\dagger(0) \rangle \end{pmatrix}.$$

The excitonic gap $\Delta_{\sigma\sigma'}$ is related to the off-diagonal Green's function

$$\Delta_{\sigma\sigma'}(\mathbf{k}) = \sum_q V(\mathbf{k} - \mathbf{q}) \mathcal{G}_{ab}^{\sigma\sigma'}(\mathbf{q}, \tau = 0^-). \qquad (6)$$

Ignoring for the moment the possibility of ferromagnetic ordering, the MF Green's function is given by

$$\mathcal{G}^{\sigma\sigma'}(\mathbf{k}, i\omega) = -\left(-i\omega + g_k - \mu + \epsilon_k \tau^z + \frac{\Delta_{\sigma\sigma'}}{2}(\tau^x - i\tau^y) \right. $$
$$\left. + \frac{\Delta_{\sigma'\sigma}^*}{2}(\tau^x + i\tau^y) \right)^{-1}, \qquad (7)$$

where $\epsilon_k = (\epsilon_k^a - \epsilon_k^b)/2$ and $g_k = (\epsilon_k^a + \epsilon_k^b)/2$ and $\vec{\tau}$ are Pauli matrices in the band space. Equation (7) must be solved in conjunction with the gap equation [Eq. (6)] to obtain a self-consistent solution. At this point, it is convenient to introduce the decomposition of $\Delta_{\sigma\sigma'}$ in terms of the singlet Δ_s and triplet $\vec{\Delta}_t$ order parameters

$$\Delta_{\sigma\sigma'} = (\Delta_s \mathcal{I} + \vec{\Delta}_t \cdot \vec{\sigma})_{\sigma\sigma'}, \qquad (8)$$

where $\mathcal{I}$ and $\vec{\sigma}$ are the 2×2 unit and Pauli matrices in the spin space, respectively. Because the Hamiltonian H_{DT} is invariant under separate rotations of the valence and conduction electrons, the triplet states are degenerate with singlet states. Consider the case where the order parameter is collinear with the spin, i.e., $\vec{\Delta}_t = \Delta_t \hat{z}$. With this replacement, the MF Hamiltonian decouples the spin-up and spin-down electrons. It is straightforward to obtain the one-particle excitation spectrum of spin $\sigma(=\pm)$ electrons

$$\xi_{k\sigma}^\pm = -\mu + g_k \pm \sqrt{\epsilon_k^2 + \Delta_\sigma^* \Delta_\sigma}, \qquad (9)$$

where $\Delta_\sigma = \Delta_s + \sigma \Delta_t$. In the theory of excitonic insulator, it is often assumed that the electronic dispersion relation are nested and isotropic, i.e., $\epsilon_k^a = -\epsilon_k^b$. As made apparent in Eq. (7), the particle-hole transformation $b_k \to b_{-k}^\dagger$ maps the prob-

lem onto two copies of the BCS model in a Zeeman field (a copy for each spin polarization). The Zeeman field takes the role of the chemical potential. This problem has been worked out, within a MF treatment, in Refs. 15 and 16. Assuming a strong screening of the Coulomb interaction, i.e., $V(\mathbf{k}) \approx V_0$, we see from Eq. (6) that the gap equation becomes momentum independent. At stoichiometry, we obtain a BCS-like state with a gap $|\Delta_\sigma| = \Delta_0 \equiv 2t \exp(-1/N_0 V_0)$, where t is a cutoff energy around the Fermi surface and N_0 is the density of states per spin at the Fermi level. The lower band ξ^- is fully occupied whereas the upper band ξ^+ is empty: the system is an excitonic insulator with a one-particle excitation gap of Δ_σ. Turning on the chemical potential, the hole and electron Fermi surfaces shift with respect to one another. This loss of nesting lowers the condensation energy and ultimately the excitonic state disappears. For a uniform order parameter, the transition occurs at $\mu = \mu_c \equiv \Delta_0/\sqrt{2}$ via a first-order transition. The condensation energy per spin direction relative to the normal state for $\mu < \mu_c$, is

$$\Delta E_\sigma(\mu) = N_0 \left(\mu^2 - \frac{\Delta_0^2}{2} \right). \quad (10)$$

At $\mu = \mu_c$, the ground state is degenerate and *each* spin polarization can be in a state where $\Delta = 0$ or $\Delta = \Delta_0$. Although the ground state has generally a twofold degeneracy at a first-order transition point, the degeneracy for *each* spin species is nongeneric. Up to this point, the MF treatment has neglected the effect of the intraband Coulomb interaction. While it is appropriate to ignore the effect of the direct part of the Coulomb interaction for uniform states, its exchange part yields a ferromagnetic interaction. The spin of the electrons in the conduction and valence bands, respectively $\vec{s}_a = a^\dagger \vec{\sigma}/2a$ and $\vec{s}_b = b^\dagger \vec{\sigma}/2b$, interact via the Heisenberg Hamiltonian $H_S = -J(\vec{s}_a^2 + \vec{s}_b^2)$ where $J > 0$. In our mean-field theory, $J = 2V_0$. However, the exchange constant tends to be poorly approximated by the direct coupling constant because the true exchange is screened by the dielectric function of the crystal. Hence we take J to be an adjustable parameter interaction (although still of order V_0). Phenomenologically, J is related to the antisymmetric Landau-Fermi liquid parameter F_0^A via the relation $J = (F_0^A/N_0)$.[17] Note that there are additional terms in the full crystal Hamiltonian that couple to the excitonic order parameter but are negligibly small compare to V_0, and hence can be safely ignored in first approximation. To take the exchange energy into account, we introduce a generalized mean-field theory, replacing $-J\vec{s}_a^2 \rightarrow -2\vec{h}_a \cdot \vec{s}_a + \vec{h}_a^2/J$, and similarly for the valence electrons. We find

$$\mathcal{G}(\mathbf{k}, i\omega) = -\left(-i\omega + g_k - \mu + \epsilon_k \tau^z + \frac{\Delta_s + \vec{\Delta} \cdot \boldsymbol{\sigma}}{2} (\tau^x - i\tau^y) \right.$$

$$+ \frac{\Delta_s^* + \vec{\Delta}^* \cdot \boldsymbol{\sigma}}{2} (\tau^x + i\tau^y)$$

$$\left. - (\vec{h}_a + \vec{h}_b) \cdot \vec{\sigma} - (\vec{h}_a - \vec{h}_b) \cdot \vec{\sigma} \tau^z \right)^{-1}, \quad (11)$$

where the self-consistent equations are
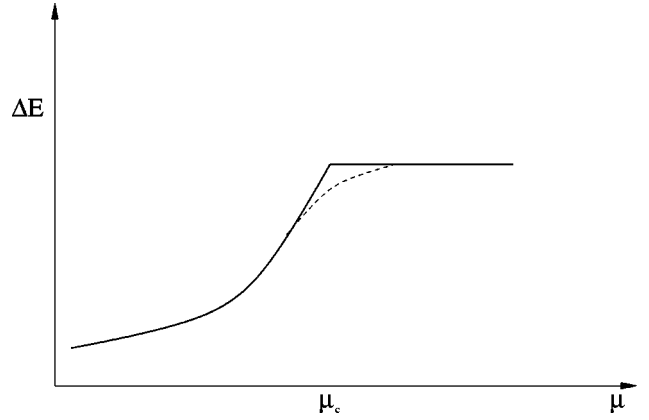
FIG. 1. Maxwell construction for the condensation energy: With the bold line, we plot Eq. (10) for the condensation energy per spin species. For the collinear order parameter, the energy gain $\Delta E(\mu + h) + \Delta E(\mu - h)$ near the first order transition is *linear* in h rather than quadratic. The dashed line shows the gain in condensation energy resulting from the exchange term.

$$\vec{h}_a = \frac{J}{2} \sum_k \text{Tr}[\vec{\sigma} \mathcal{G}_{aa}(\mathbf{k}, \tau = 0^-)],$$

$$\vec{h}_b = \frac{J}{2} \sum_k \text{Tr}[\vec{\sigma} \mathcal{G}_{bb}(\mathbf{k}, \tau = 0^-)]. \quad (12)$$

We have studied the energetics for collinear spin polarization and perfectly nested Fermi surfaces. While the spin branches are no longer decoupled, we find the condensation energy of the system ΔE_T is given by a simple Maxwell construction

$$\Delta E_T(\mu) = \Delta E_+(\mu + h) + \Delta E_-(\mu - h) + \frac{2h^2}{J}, \quad (13)$$

where $h = |\vec{h}_a| = |\vec{h}_b|$. Minimizing this functional, we find that an excitonic ferromagnet ground state is favored in a range of chemical potential $\mu_c \sqrt{1 - 2N_0 J} < \mu < \mu_c \sqrt{(1 - 2N_0 J)/(1 - 4N_0 J)}$ (see Fig. 1). This excitonic polarized state is characterized by having one spin species, say spin-up, in the normal state whereas the spin-down electrons are paired ($|\Delta_-| = \Delta_0$). One can understand the origin of the magnetism by studying its effect on the Fermi surfaces. The magnetic field favors the pairing of the spin-down electrons by increasing the coincidence of the hole and electron Fermi surfaces for the spin-down. This gain in condensate energy is *linear* in h near the first-order transition. While this redistribution of the charge carriers comes at the expense of a loss in kinetic energy for the spin-up electrons, this increase in energy is quadratic in the field therefore favoring ferromagnetic ordering.

IV. INCOMMENSURABILITY

Although the previous results are suggestive, a complete understanding of the ferromagnetism and its applicability to the hexaborides is still lacking. The large number of com-
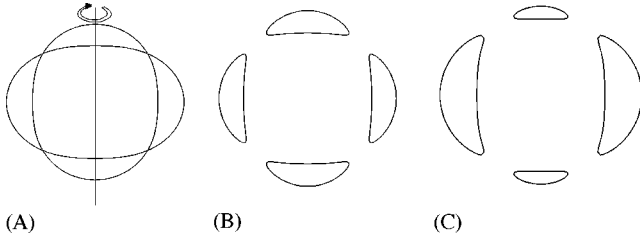
FIG. 2. Fermi-surface cut through the z-x plane, where the z axis is an axis of revolution. For noninteracting electrons, the imperfectly nested Fermi surface consists of two ellipsoids (A). In the undoped EM phase (B), the Fermi surface is partially gapped, forming a hole lens and an electron ring. Upon doping (C), the hole lens drops out, leaving an enlarged electron ring.

pounds exhibiting weak ferromagnetism discovered to this day argues for the robustness of the phenomenon. However, most of theoretical results seemingly hinge on the perfect nesting of the hole-electron Fermi surface to lead to an excitonic insulator. Moreover, the existence of a Fermi surface as seen in ARPES and dHvA data rules out this simple scenario. A crucial step to circumvent these difficulties is to realize the hole and electron bands are not related by any symmetry principle; in real materials, electron and hole Fermi surfaces are not generally perfectly nested. To study the effect of incommensurability on the excitonic states, we introduce the anisotropic dispersion relations for the valence and conduction bands:

$$\epsilon_k^a = v(|k| - k_F) + \delta v k_F \cos(2\theta) - \mu^*,$$

$$(14)$$

$$\epsilon_k^b = -v(|k| - k_F) + \delta v k_F \cos(2\theta) - \mu^*.$$

Here v is the Fermi velocity, k_F is the Fermi wave vector, δ is a dimensionless parameter that controls the degree of antinesting, and θ is the azimuthal angle. For $\delta = 0$, we recover the isotropic and nested dispersion relations, whereas for finite δ the Fermi surface is described by two non-coinciding ellipsoids (see Fig. 2). The parameter μ^* is determined by imposing charge neutrality at stoichiometry at $T = 0$, i.e.,

$$\sum_k [\Theta(-\epsilon_k^a) + \Theta(-\epsilon_k^b)] = \sum_k 1, \qquad (15)$$

where $\Theta(x)$ is the Heaviside function. This toy model characterization of the energy dispersion simply describes the effect of anisotropy, and allows us to make analytical progress. Furthermore, the large uncertainties in the available data for the effective masses and gap values did not allow for an accurate theoretical description, although local-density-approximation calculations[2] on CaB_6 would suggest δ to be positive.

Based upon our previous analysis, we consider only collinear states and minimize the energy functional,
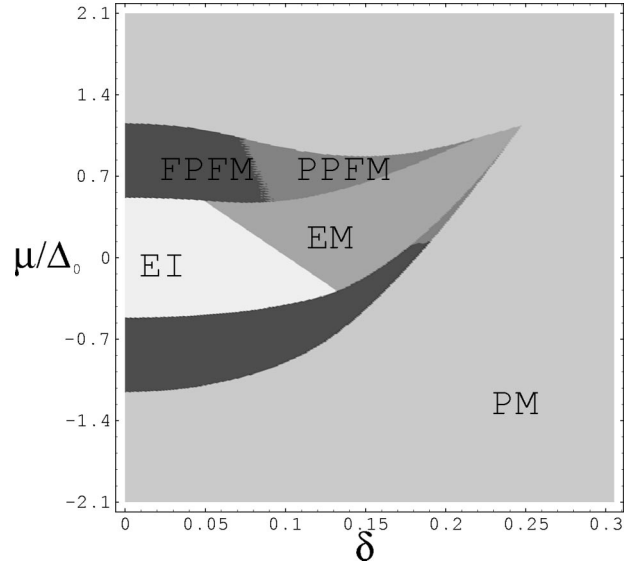
FIG. 3. Phase diagram as a function of the chemical potential μ and the antinesting parameter δ. PM indicates a paramagnetic metallic phase, EI and EM are the excitonic insulating and metallic phases, respectively. FPFM and PPFM denote the fully polarized excitonic ferromagnet and the partially polarized excitonic ferromagnet, respectively. Most phase transitions are continuous. The exceptions are the PPFM/FPFM and the EI/EM boundaries.

$$E_T[\mu] = \sum_{\alpha, \sigma = \pm} \left[\int \frac{d^3 k}{(2\pi)^3} (\xi_{k,\sigma}^\alpha - \sigma h) \Theta(-\xi_{k,\sigma}^\alpha + \sigma h) \right]$$

$$+ \frac{2h^2}{J} + \frac{\Delta_+^2 + \Delta_-^2}{V_0}, \qquad (16)$$

where $\xi_{k,\sigma}^\alpha$ is the energy eigenvalue determined in Eq. (9). The integral over wave vectors can be expressed in terms of elliptical functions. From the three parameters (h, Δ_+, Δ_-) minimization search, we have determined the phase diagram at zero temperature as a function of μ, the chemical potential and δ, the antinesting parameter (See Fig. 3). Not surprisingly, for small values of δ, we find that the system behaves analogously to the nested case. At stoichiometry, the system is in the excitonic insulating (EI) phase. Increasing the chemical potential, the EI state becomes unstable to a ferromagnetic phase before disappearing into the normal state via a first-order transition. However, larger values of δ allows for the possibility of gapless excitations in the one-particle excitation spectrum. Hence, while the excitonic metal exhibits a nonzero order parameter, i.e., $(\Delta_s = 0, \Delta_t \neq 0,$ or $\Delta_t = 0, \Delta_s \neq 0)$, the presence of an incompletely gapped Fermi surface modifies radically its electronic properties. To illustrate this point, we have calculated the electronic density of states (DOS),

$$N(\omega) = -\frac{1}{2\pi} \text{Im} \sum_k \text{Tr}[\mathcal{G}(\mathbf{k}, \omega)], \qquad (17)$$

at stoichiometry in the insulating and metallic phases. As shown in Fig. 4, in spite of the excitonic ordering, the DOS in the metallic phase does not show the typical shoulder edge
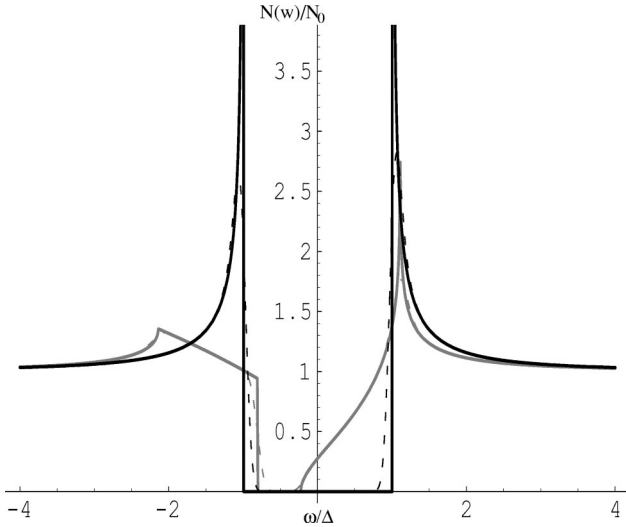
FIG. 4. Electronic density of states (DOS): The DOS is in the excitonic insulator and metal phases are indicated by black and gray lines, respectively. The dashed lines represent the DOS in the presence of scattering for values of $\gamma/\Delta = 0.1$ (see the text).

FIG. 5. Electromagnetic absorption as a function of frequency ω in the EM phase. The optical edge near 2Δ is smeared by scattering processes.

present in the insulating excitonic phase. The EM/EI transition is continuous and the excitonic gap varies smoothly across the transition line defined by $\mu = \mu_t$. However, the metallic instability is signaled by the density of states at the Fermi level, which show a singular behavior across the transition line, increasing as $\sqrt{\mu - \mu_t}$. The introduction of charge carriers in the EM phase raises the Fermi level, leading to changes in the topology of the Fermi surface. Recent results on dHvA experiments on divalent hexaborides have observed quantum oscillations in La-doped CaB_6.[13,14] These oscillations have been interpreted as due to the presence of Fermi sheets in the undoped compounds.[13] The Fermi surface is thought to consist of two pieces, an electron ring, and a hole lens centered around the X point in the Brillouin zone. In the La-doped CaB_6, dHvA data show the hole pocket dropping out, yielding a single electron sheet. These results are consistent with our model. As seen in Fig. 2, in the undoped case, the Fermi surface is gapped at the intersection of the hole and electron Fermi surface, leaving two Fermi sheets, a ring and a lens. For positive values of δ, the lens and ring are holelike and electronlike, respectively. As electrons are added to the system, the hole pocket shrinks and eventually becomes gapped out due to the excitonic gap, leaving a single electron ring, consistent with experimental data. However, further experiments on cleaner samples are needed to clearly determine the topology of the Fermi surface.

An upshot of the finite density of states at the Fermi level is the possibility of distributing the extra carriers asymmetrically between spin species. As shown in Fig. 5, the EM phase gives way to a *partially* polarized ferromagnet where the extra carriers carry only a *fraction* of a Bohr magneton. When δ becomes of the order of Δ/ϵ_F, the incommensurability of the hole and electron Fermi surfaces becomes too large and hinders the gap formation. However, this state may be itself unstable to the formation of nonhomogeneous states with spin- and/or charge-density waves.[6]
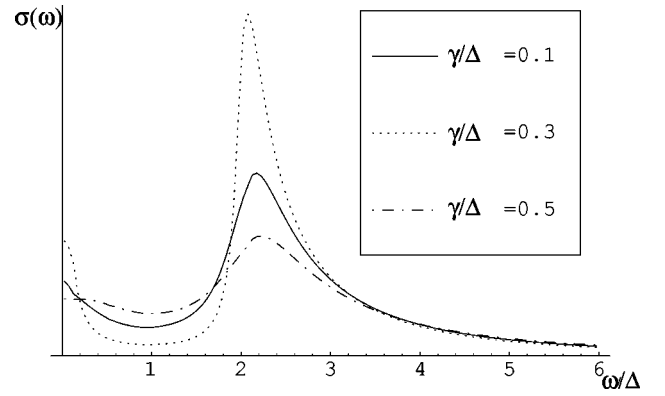
The result of our calculation of the magnetic moment per dopant for the doped excitonic metal is shown in Fig. 6. In contrast to the case of a doped excitonic insulator, the ferromagnetic moment per carrier is smaller than a Bohr magneton due to the electrons spilling over both branches of the spin species. It is interesting to note that the magnetic moment can be further reduced by having an order parameter noncollinear with the spin.[2] At this level of approximation, these states are degenerate, but the terms that break the $SU(2) \times SU(2)$ explicitly will determine the orientation of the order parameter in the spin space. However, whichever state is eventually favored, our result provides an upper bound constraint for the magnetic moment.

Unlike in the EI/FPFM transition, the electronic charge density can in principle evolve smoothly across the EM/PPFM boundary, thus one might expect a second-order (con-
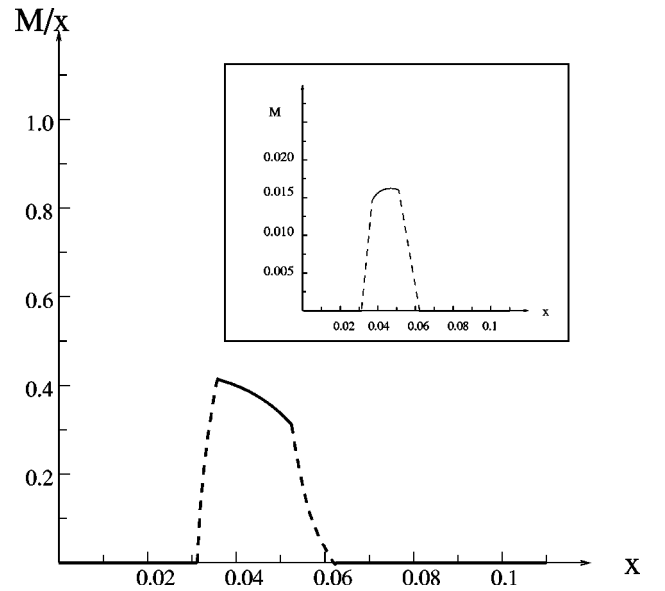
FIG. 6. Magnetic moment in Bohr magneton per unit carrier as a function of doping at $T = 0$ for $\delta = 0.15$. In the phase separation regime, represented by the dashed line, we expect the magnetization density to vary linearly between the two competing phases, as shown in the inset.

tinuous) transition to arise. However, we find in MFT a first-order transition. Moreover, we suspect this may be a general result due to singular quasiparticle-mediated interactions. An argument in favor of a first-order transition is found by considering the system at low but non-zero temperature. In the neighborhood of the transition, were it second order, it should be possible to develop a Landau expansion of the free energy in terms of the magnetic order parameter h, with Δ already nonzero. This expansion must be analytic at $T>0$

$$F(\mu,h)=F(\mu,0)+Ah^2+Bh^4+\cdots. \tag{18}$$

Parameters A and B are related to two- and four-point spin correlation functions respectively. As $T\rightarrow0$, we find $A=(2/J)-4N_0(\mu)$ and $B\rightarrow-\infty$, hence precluding the validity of such an expansion and therefore of a continuous transition. It would be desirable to develop a proper field-theoretic argument posed directly at $T=0$. A consequence of a direct first-order transition is a discontinuous jump of the electronic density across the boundary line. Since experiments are performed at fixed charge density, phase separation occurs for a range of doping. However, the long-range Coulomb interaction will likely frustrate macroscopic phase separation and an inhomogeneous state is expected.[18]

V. ELECTROMAGNETIC ABSORPTION

A powerful technique that can be used to probe the excitonic state is the infrared optical conductivity. Just as for superconductors, the excitonic insulator signature on the optical conductivity is the suppression of absorption for frequencies twice below the excitonic gap Δ_0. However, one of the puzzling aspects of optical conductivity measurements on the undoped hexaborides is the absence of a hard optical gap and a strong doping dependence.[19] One expects the presence of gapless quasiparticles in the excitonic metal state to be responsible for this result. To investigate this issue quantitatively, we calculate the optical conductivity tensor $\sigma_{\mu\nu}(\omega)$ which is related to the current-current correlation function $\Pi_{\mu\nu}$,

$$\sigma_{\mu\nu}(\omega>0)=\frac{-1}{\omega}\text{Im}\int_{-\infty}^{\infty}dt\, e^{i\omega t}\Pi_{\mu\nu}(t), \tag{19}$$

where $\Pi_{\mu\nu}(t)=-i\Theta(t)\langle[J_\mu(t),J_\nu(0)]\rangle$ and $\vec{J}$ is the current operator. The Greek indices refer to the spatial components. We calculate the correlation function in the Matsubara formalism, and obtain the desired retarded function by an analytical continuation. To allow for electronic scattering due to impurities and/or lattice imperfections, we introduce a finite lifetime to the quasiparticle by performing the substitution $\omega\rightarrow\omega+\gamma\,\text{sgn}(\omega)$ in the Green's function

$$\mathcal{G}^{\sigma\sigma'}(\mathbf{k},i\omega)=\frac{\delta_{\sigma\sigma'}}{i\omega+i\gamma\,\text{sgn}(\omega)-\mu+g_k+\epsilon_k\tau^z+\Delta_\sigma\tau^x}, \tag{20}$$

where, for concreteness, we consider a pure triplet order parameter. Ignoring vertex corrections to the conductivity, the correlation function is given by the bubble diagram

$$\Pi_{\mu\nu}(i\omega)=e^2\int\frac{d\Omega}{2\pi}\frac{d^3k}{(2\pi)^3}\text{Tr}[\mathcal{G}(\mathbf{k},i\Omega-i\omega/2)v_\mu\mathcal{G}(\mathbf{k},i\Omega$$
$$+i\omega/2)v_\nu], \tag{21}$$

where $v_\mu=\partial_\mu(\epsilon_k\tau^z-g_k)$ is the velocity of the quasiparticles. In order to evaluate the correlation function, we use the standard spectral representation for the Green's function:

$$\mathcal{G}^{\sigma\sigma'}(\mathbf{k},i\omega)$$
$$=\int\frac{d\rho}{2\pi}\frac{1}{\rho-i\omega}2\,\text{Im}\left[\frac{\delta_{\sigma\sigma'}}{\rho+i\gamma-\mu+g_k+\epsilon_k\tau^z+\Delta_\sigma\tau^x}\right]. \tag{22}$$

In the physical regime where the scattering rate γ is much smaller than Δ, the imaginary part of the correlation function in real frequencies is given by

$$\text{Im}[\Pi_{\mu\nu}(\omega)]$$
$$=\sum_\sigma\delta_{\mu\nu}\frac{(ev_F)^2}{3}\int\frac{d^3k}{(2\pi)^3}\frac{2\gamma}{\omega^2+\gamma^2}\frac{1}{4\chi^2+\gamma^2}$$
$$\times\left[[\Theta(\xi_\sigma^+)-\Theta(\xi_\sigma^++\omega)-\Theta(\xi_\sigma^-)+\Theta(\xi_\sigma^--\omega)]\right.$$
$$\times\frac{(2\chi^2)[\chi^2+(\chi+\omega)^2]+4\chi(\chi+\omega)(\chi^2-2\Delta^2)}{(\omega+2\chi)^2+\gamma^2}$$
$$\left.-(\omega\rightarrow-\omega)\right], \tag{23}$$

where $\chi=\sqrt{\epsilon_k^2+\Delta^2}$. We evaluate the correlation in different limits. For low frequencies, i.e., $\omega\ll\Delta$, we find a Drude-like conductivity

$$\sigma_{\mu\nu}(\omega)=\delta_{\mu\nu}\frac{(ev_F)^2\gamma}{\omega^2+\gamma^2}n, \tag{24}$$

where

$$n=\frac{1}{3}\sum_{\sigma=\pm}\sum_{\alpha=\pm}\int\frac{d^3k}{(2\pi)^3}\frac{\epsilon_k^2}{\epsilon_k^2+\Delta_\sigma^2}\delta(\xi_{k,\sigma}^\alpha). \tag{25}$$

Hence the scattering of gapless excitations generates absorption in the low-energy sector of the optical conductivity. For high frequencies, the dominant contribution to the integral comes from exciton pair breaking, i.e., when $\omega\simeq2\chi$. Thus, for $\omega\ll\gamma$,

$$\sigma_{\mu\nu}(\omega)=4\delta_{\mu\nu}\sum_\sigma\frac{(ev_F\Delta_\sigma)^2}{\omega^3}$$
$$\times\int\frac{d^3k}{(2\pi)^3}\frac{2\gamma}{(\omega-2\chi)^2+\gamma^2}[\Theta(\xi_{k,\sigma}^+)-\Theta(\xi_{k,\sigma}^+)]. \tag{26}$$

In the clean limit, the threshold for exciton pair breaking is given by 2Δ. In this case the absorption peak shows a square root singularity $\sim\sqrt{1/(\omega^2-4\Delta^2)}$ near the threshold due to

the large amount of phase space available in k space. However, in the presence of scattering, the wave vector k is no longer a good quantum number and the peak is smeared out on a width of order γ (see Fig. 5). We conjecture that the absence of hard optical gaps in experimental data is due to metallicity and scattering that shifts the absorption to lower frequencies. Note that, because the order parameters for the spin-up and spin-down is generally different in the ferromagnetic state in clean materials, the absorption peak would be split into two peaks upon entering the ferromagnetic phase. Its experimental observation in the hexaboride materials would provide considerable support for the theory of excitonic ferromagnet.

VI. CONCLUSION

Excitonic ordering near a semiconductor-metal transition offers a natural explanation for weak ferromagnetism in the doped hexaborides. We have generalized previous studies on the excitonic ferromagnet by considering the effect of imperfect nesting on the excitonic state. Adding this significant ingredient, we showed that a phase, the excitonic metal, is stable and can account for the Fermi surface seen in the hexaborides. A ferromagnetic instability still occurs in the excitonic metal near the first-order transition. Furthermore, the small ferromagnetic moment observed in lightly doped hexaborides is naturally explained as a result of compensated moments on the imperfectly gapped Fermi surface. Although this model qualitatively explains experiments, further studies will be needed to determine the effect of the gapless excitations on the electronic transport and thermodynamic properties of the system.

[1] D. P. Young, D. Hall, M. E. Torelli, Z. Fisk, J. L. Sarrao, J. D. Thompson, H. R. Ott, S. B. Oseroff, R. G. Goodrich, and R. Zysler, Nature (London) **397**, 412 (1999).

[2] M. E. Zhitomirsky, T. M. Rice, and V. I. Anisimov, Nature (London) **402**, 251 (1999).

[3] T. Jarlborg, Phys. Rev. Lett. **85**, 186 (2000).

[4] L. Balents and C. M. Varma, Phys. Rev. Lett. **84**, 1264 (2000).

[5] C. O. Rodriguez, R. Weht, and W. E. Pickett, Phys. Rev. Lett. **84**, 3903 (2000).

[6] V. Barzykin and L. P. Gorkov, Phys. Rev. Lett. **84**, 2207 (2000).

[7] T. Ichinomiya, Phys. Rev. B **63**, 045113 (2001).

[8] B. I. Halperin and T. M. Rice, Solid State Phys. **21**, 115 (1968).

[9] S. Massida, A. Continenza, T. M. de Pascale, and R. Monnier, Z. Phys. B: Condens. Matter **102**, 83 (1997).

[10] However, recent calculations based on the *GW* approximation reported the formation of a rather large band gap; see H. J. Tromp, P. van Gelderen, P. J. Kelly, G. Brocks, and P. A. Bobbert, Phys. Rev. Lett. **87**, 016401 (2001); J. D. Denlinger, J. A. Clack, J. W. Allen, G.-H. Gweon, D. M. Poirier, C. G. Olson, J. L. Sarrao, A. D. Bianchi, and Z. Fisk, cond-mat/0107429 (unpublished).

[11] B. A. Volkov, Yu. V. Kopaev, and A. I. Rusinov, Zh. Eksp. Teor. Fiz. **68**, 1899 (1975) [Sov. Phys. JETP **41**, 952 (1975)].

[12] J. D. Denlinger, J. A. Clack, J. W. Allen, G.-H. Gweon, D. M. Poirier, C. G. Olson, J. L. Sarrao, and Z. Fisk, cond-mat/0009022 (unpublished).

[13] D. Hall, D. P. Young, Z. Fisk, T. P. Murphy, E. C. Palm, A. Teklu, and R. G. Goodrich, Phys. Rev. B **64**, 233105 (2001).

[14] T. Terashima, C. Terakura, Y. Umeda, N. Kimura, H. Aoki, and S. Kunii, J. Phys. Soc. Jpn. **69**, 2423 (2000).

[15] A. I. Larkin and Yu. N. Ovchinnikov, Zh. Eksp. Teor. Fiz. **47**, 1136 (1964) [Sov. Phys. JETP **20**, 762 (1965)].

[16] P. Fulde and R. A. Ferrel, Phys. Rev. A **135**, A550 (1964).

[17] A. A. Abrikosov, L. P. Gorkov, and I. E. Dzyaloshinski, in *Methods of Quantum Field Theory in Statistical Physics* (Prentice-Hall, Englewood Cliffs, NJ, 1963).

[18] L. Balents, Phys. Rev. B **62**, 2346 (2000).

[19] P. Vonlanthen, E. Felder, L. Degiorgi, H. R. Ott, D. P. Young, A. D. Bianchi, and Z. Fisk, Phys. Rev. B **62**, 10 076 (2000).